Electronic and magnetic properties of perovskite selenite and tellurite compounds: $CoSeO_3$, $NiSeO_3$, $CoTeO_3$, and $NiTeO_3$

A. Rafi M. Iasir,[1,*] Todd Lombardi,[2,*] Qiangsheng Lu,[2,*] Amir M. Mofrad,[3,*] Mitchel Vaninger,[2,*] Xiaoqian Zhang,[2,4,*] and David J. Singh[2,5,†]

[1]*Nuclear Engineering Program, University of Missouri, Columbia, Missouri 65211, USA*
[2]*Department of Physics and Astronomy, University of Missouri, Columbia, Missouri 65211-7010, USA*
[3]*Department of Biomedical, Biological and Chemical Engineering, University of Missouri, Columbia, Missouri 65211, USA*
[4]*Jiangsu Provincial Key Laboratory of Advanced Photonic and Electronic Materials, Collaborative Innovation Center of Advanced Microstructures, School of Electronic Science and Engineering, Nanjing University, Nanjing 210093, China*
[5]*Department of Chemistry, University of Missouri, Columbia, Missouri 65211, USA*

(Received 11 August 2019; revised manuscript received 21 November 2019; published 9 January 2020)

Selenium and tellurium are among the few elements that form ABO_3 perovskite structures with a four valent ion in the A site. This leads to highly distorted structures and unusual magnetic behavior. Here we investigate the Co and Ni selenite and tellurite compounds, $CoSeO_3$, $CoTeO_3$, $NiSeO_3$, and $NiTeO_3$, using first principles calculations. We find an interplay of crystal field and Jahn-Teller distortions that underpin the electronic and magnetic properties. While all compounds are predicted to show an insulating G-type antiferromagnetic ground state, there is a considerable difference in the anisotropy of the exchange interactions between the Ni and Co compounds. This is related to the Jahn-Teller distortion. Finally, we observe that these four compounds show characteristics generally associated with Mott insulators, even when described at the level of standard density functional theory. These are then dense bulk insulators that are correctly described as insulators in a standard band structure picture but that satisfy the common experimental criteria to classify them as Mott-type insulators.

DOI: 10.1103/PhysRevB.101.045107

I. INTRODUCTION

Perovskite oxides constitute an exceptionally broad class of compounds, and exhibit many diverse properties and useful functionalities [1,2]. This includes high temperature superconductors [3], widely used ferroelectric and piezoelectric materials [4], colossal magnetoresistive compounds [5,6], ionic conductors [7], and many other important materials. The structure type is characterized by an ABO_3 stoichiometry, based on corner linked BO_6 octahedra arranged on a simple cubic lattice, often distorted. These distortions are key to the chemical flexibility of the perovskite structure. For example, A-site ions that are too small for the site can be accommodated by coordinated tilting of the corner linked BO_6 octahedra, thus allowing small ions to be inserted, and at the same time providing a chemical tuning mechanism for modulating the bond angles and properties that depend on them. The chemical and structural tunability of this structure type also leads to fascinating physics including quantum critical phenomena, Mott and other metal insulator transitions, and magnetoelectric materials. The manganites in particular, but other materials as well, have also highlighted the importance of coupling between structure and electronic properties in perovskites [2,5,8–10]. In this regard, investigation of compounds with unusual perovskite chemistry or structure is useful in understanding the range of possible behaviors.

Here we investigate the cobalt and nickel containing selenite and tellurite compounds, $CoSeO_3$, $CoTeO_3$, $NiSeO_3$, and $NiTeO_3$. These compounds, although known since the 1970s [11–13], have been relatively little studied. These are highly unusual perovskites. In particular, they have extremely strong distortions leading to very strong deviation of the metal-O-metal bond angles from the ideal value of 180° and they have exclusively divalent cations at the perovskite B site, while normally only partial occupancy of divalent B-site ions, counterbalanced by higher valence ions on other B sites, can occur in perovskites. This is as rationalized by the Pauling rules [14], in which the corner sharing perovskite structure is stabilized by repulsion between highly charged B-site ions. Here, the unusual structures are presumably stabilized by covalent interactions between O and the Se or Te, leading to a chemistry intermediate between, on the one hand, normal ionic perovskite crystals, in this case stabilized by strong off-centering and lone pair activity of the very small Se^{4+} and Te^{4+} ions, and, on the other hand, salts based on complex anions [12], specifically, $(SeO_3)^{2-}$ or $(TeO_3)^{2-}$.

It is known that $CoSeO_3$, $CoTeO_3$, $NiSeO_3$, and $NiTeO_3$ all have magnetic ground states. While transport data and spectroscopy have not been reported, based on their reported colors [12] they are probably insulating. Unlike $MnSeO_3$, insulating behavior in these compounds is not an obvious result from electron counting. The corresponding Cu compounds show a strong dependence of magnetic order on

*These authors contributed equally.
†singhdj@missouri.edu

structure, including a crossover from antiferromagnetic to ferromagnetic behavior as the bond angle is distorted in the $CuTeO_3$–$CuSeO_3$ alloy system [15].

Remarkably, in the present study we find all four of these materials to exhibit an unusual type of insulating character, specifically they are predicted to be band insulators at the PBE level both in their ground state and in all configurations tested. The paramagnetic state for a local moment system will consist of disordered moments, with no long range order and a temperature dependent degree of short range order. Based on the fact that we find insulating behavior independent of the magnetic order, we infer that these compounds at the level of standard approximate density functionals will be insulating in the disordered paramagnetic state. This is a characteristic of Mott-type insulators, and so they may be called Slater-Mott-type insulators.

II. METHODS AND STRUCTURE

The calculations presented here were done in the framework of density functional theory (DFT) using the general potential linearized augmented plane wave (LAPW) method [16] as implemented in the WIEN2K code [17]. We used the generalized gradient approximation (GGA) of Perdew, Burke, and Ernzerhof (PBE) [18]. We tested different Brillouin zone samplings and did calculations with different choices of LAPW sphere radii. The main results shown here were obtained with a Brillouin zone sampling consisting of $8 \times 8 \times 6$ uniform meshes and LAPW sphere radii of 1.8 Bohr for Ni, Co, Se, and Te, and 1.4 Bohr for O. The LAPW plus local orbital basis sets were used with plane wave sector cutoffs, $K_{\max}$, determined by the criterion $R_{\min}K_{\max} = 7$, where $R_{\min}$ is the smallest, i.e., the O, sphere radius. This leads to an effective value of 9 for the metal, Se, and Te atoms. Local orbitals were employed for the semicore states of the transition elements, including the $3s$ and $3p$ states, as well as the d semicore states of Te and Se, and s semicore state of Te. We also included a local orbital for the O $2s$ level. These are settings for a highly converged basis.

The four compounds studied are all reported to occur in an orthorhombic *Pnma* (space group 62) structure with four formula units per unit cell. This is a very common perovskite variant. However, they are unusual in the size of the distortions from the ideal cubic structure, which are extremely large in these materials. Our calculations are based on the experimental lattice parameters. The internal atomic coordinates in the unit cells were determined by total energy minimization with a ferromagnetic ordering. This was done by relaxing the positions until the calculated forces on all atoms were less than 2 mRy/Bohr. We also did calculations for antiferromagnetic orderings. However, the calculated forces remained small independent of the specific ordering pattern. In the worst case, this amounted to 5.8 mRy/Bohr. Thus we conclude that relaxation based on ferromagnetic ordering is sufficient. For the Co compounds, which may be particularly sensitive to structure, we also fully relaxed the atomic positions with G-type order. This led to further stabilization of the G-type magnetic structure by 2.0 meV/f.u. for $CoSeO_3$ and 1.7 meV/f.u. for $CoTeO_3$. Of course it is not possible to absolutely establish a ground state without testing all possible configurations for all possible relaxed structures. We also did relaxation of the atomic positions for the Co compounds imposing no symmetry other than inversion. However, we did not find any additional distortion from this calculation.

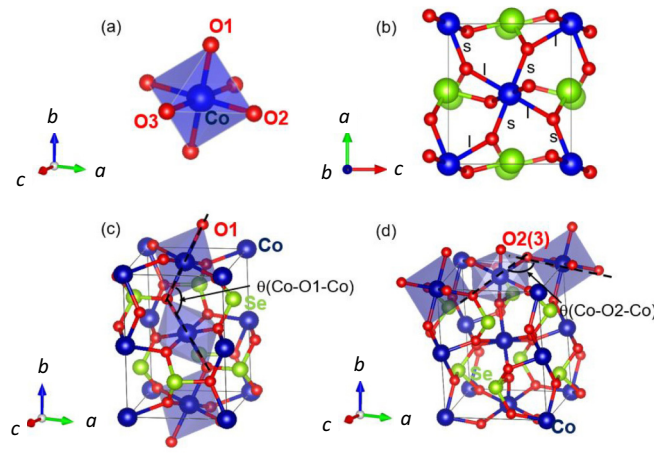

FIG. 1. Crystal structure of *Pnma* orthorhombic $CoSeO_3$. (a) CoO_6 octahedron, (b) view along b axis, (c) arrangement of octahedra in ac plane, and (d) view showing bond angles due to octahedral rotation.

The structure of $CoSeO_3$, which is representative, is depicted in Fig. 1. The calculated structural data is summarized in the Supplemental Material, Table S1 [19]. As seen, the structures, while perovskite in nature with the characteristic motif of corner sharing MO_6 octahedra, are very strongly distorted from the cubic perovskite structure. This is evident also in the reported experimental lattice parameters, which deviate from the pseudocubic relationship, $a = c = \sqrt{2}a^*$, $b = 2a^* = \sqrt{2}a$, where a^* is the effective cubic lattice parameter. The Co compounds have larger lattice parameters and bond lengths than the corresponding Ni compounds. This simply reflects the larger ionic radius of high spin Co^{2+} compared to high spin Ni^{2+} [20]. Within the structure, all four MO_6 octahedra are equivalent, and from the perspective of the octahedra and their connectivity, the local structure is characterized by three metal-O bond lengths and two metal-O-metal bond angles, as illustrated in Figs. 1(a), 1(c), and 1(d). Specifically, as illustrated, the three angles are Co-O1-Co, Co-O2-Co, and Co-O3-Co, but Co-O2-Co and Co-O3-Co are the same (O1 is the connection to the Co along the b axis, while O2 and O3 are the O that connect in the ac-plane directions). These parameters are given in Table I, along with an octahedral

TABLE I. Structural parameters of the four compounds, based on the relaxed atomic positions (see text and Fig. 1). M is the metal atom (Co or Ni).

	$CoSeO_3$	$NiSeO_3$	$CoTeO_3$	$NiTeO_3$
M-O1 (Å)	2.129	2.110	2.079	2.072
M-O2 (Å)	2.211	2.146	2.287	2.189
M-O3 (Å)	2.056	2.058	2.082	2.101
θ (M-O1-M)	126.2°	126.1°	129.2°	129.6°
θ (M-O2-M)	131.3°	132.0°	133.7°	134.6°
Δ_d	0.00088	0.00030	0.00205	0.00055

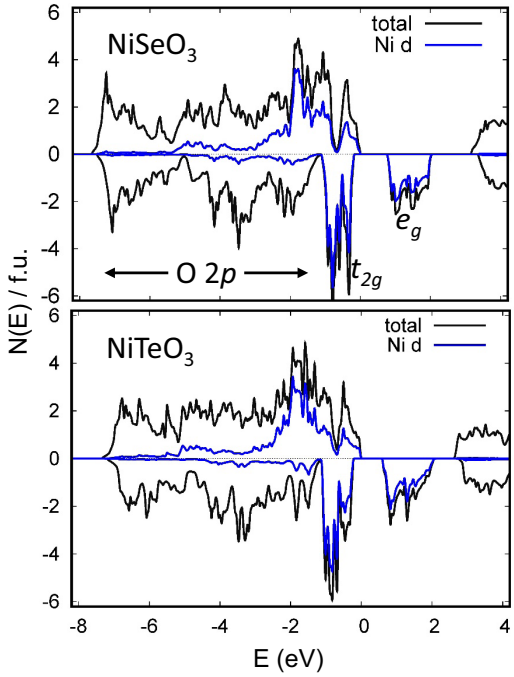

FIG. 2. Electronic density of states and Ni d projections for non-ground-state ferromagnetic ordering for $NiSeO_3$ and $NiTeO_3$. The projects are onto the LAPW spheres. The energy zero is at the highest occupied state.

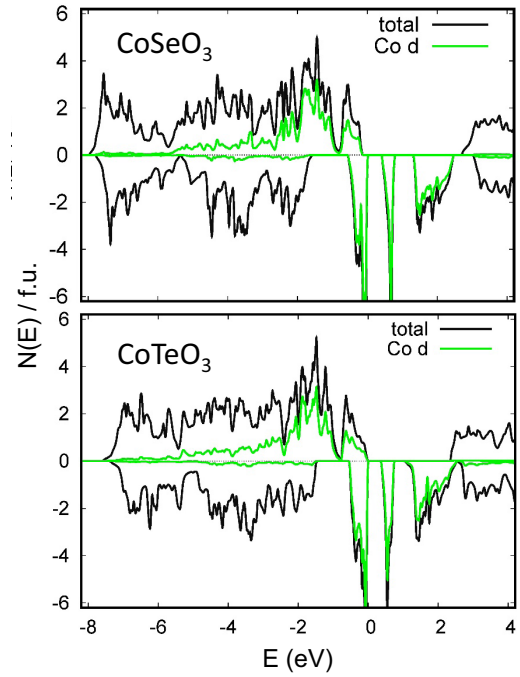

FIG. 3. Electronic density of states and Co d projections for non-ground-state ferromagnetic ordering for $CoSeO_3$ and $CoTeO_3$.

distortion parameter [21],

$$\Delta_d = \frac{1}{6}\sum_{n=1,6}\left[\frac{d_n - d}{d}\right]^2, \tag{1}$$

where the d_n are the six metal–O distances in an octahedron and d is the average. This distortion parameter was previously used in the analysis of Jahn-Teller splittings in manganites [21]. As seen, the bond angles characterizing the octahedral rotation are similar for the four compounds, and are slightly lower (corresponding to stronger rotation) for the selenite compounds, consistent with the smaller size of Se^{+4} compared to Te^{+4}. The distortion of the octahedra on the other hand is sensitive to the metal atom, and is substantially larger for the Co compounds as compared to the corresponding Ni compounds.

III. ELECTRONIC STRUCTURE

As mentioned, the structure relaxation was done using an assumed ferromagnetic ordering and the standard PBE GGA density functional. Ferromagnetic solutions were found for all four compounds (note that as discussed below there are lower energy antiferromagnetic orderings). The calculated electronic densities of states are shown along with projections in Figs. 2 and 3. Remarkably all the compounds are insulating with this ferromagnetic ordering. This is similar to what was found previously for $MnSeO_3$, which has the d^5 ion Mn^{2+}, forming a high spin antiferromagnetic insulating ground state [22,23]. The spin magnetizations are $3\mu_B$ per formula unit for $CoSeO_3$ and $CoTeO_3$ and $2\mu_B$ per formula unit for the Ni compounds, $NiSeO_3$ and $NiTeO_3$.

The electronic structure of the four compounds in the valence energy range consists of occupied O $2p$ derived bands from ~ -7 eV to ~ -1 eV, with respect to the energy zero, which is set to the highest occupied state. The chalcogen s states are shown below the window. The transition metal states show strong exchange splittings, as seen. Additionally, there is a strong spin dependent hybridization between the O $2p$ states and the transition metal d states. The spin dependence is seen in the differences in shape of the majority and minority d character in Figs. 2 and 3. It arises from the fact that the majority d states overlap the top of the O $2p$ bands, while the minority d states are mainly above the $2p$ bands. However, while the minority spin shows weaker hybridization than the majority, the hybridization is substantial in both spin channels. This is evident from the sizable crystal field splitting of the minority spin d states, which amounts to $\sim$2 eV for both the Co and Ni compounds (note that in transition metal oxides crystal field splitting is due to metal-ligand hybridization). The nominally unoccupied p states of Se and Te occur above the transition metal bands starting at $\sim$3 eV for the Ni compounds and $\sim$2 eV for the Co compounds. These are formally the antibonding combinations of O $2p$ and Se/Te p states from the $(SeO_3)^{2-}$ and $(TeO_3)^{2-}$ complex anions within a view of the crystal structure as a salt.

The insulating nature of the Ni compounds can be understood in a standard crystal field scheme. In an octahedral environment the $3d$ states are crystal field split into a lower lying t_{2g} manifold with three states per spin and a higher e_g manifold with two states per spin. The eight $3d$ electrons of Ni^{2+} suffice to fill the majority spin d levels plus the minority spin t_{2g} level. This then can lead to insulating behavior provided that the bandwidths are narrow enough to leave clean gaps between the minority spin t_{2g} and e_g

crystal field levels. This is evidently the case in ferromagnetic $NiSeO_3$ and $NiTeO_3$ as can be seen from Fig. 2. It should be noted, however, that this is unusual, since ferromagnetic ordering is particularly favorable for hopping and therefore is the ordering that typically has the largest bandwidths in oxides. For example, as pointed out by Slater [24], it is possible to have insulating gaps in antiferromagnetic systems due to band structure effects. This includes the prototypical Mott insulator, NiO [25]. However, the insulating character of NiO in this band structure point of view depends crucially on the particular magnetic order. In contrast, in the present case the bands are exceptionally narrow leading to narrow crystal field split levels. Thus the crystal field splitting is not washed out, even with ferromagnetic order. This is a consequence of the highly distorted perovskite structure that includes very strongly bent metal-O-metal bonds.

More remarkably, we find that both $CoSeO_3$ and $CoTeO_3$ have insulating gaps with ferromagnetic order. Co^{2+} has one less electron than Ni^{2+}. This means that there are only two minority spin electrons. As a result, there is one hole in the t_{2g} crystal field level. Such partial filling of the t_{2g} level should normally lead to a metallic state, especially with ferromagnetic order. However, in the Co compounds, unlike the corresponding Ni compounds, we find a clean gap in the minority spin t_{2g} levels at 2/3 filling. This is a Jahn-Teller splitting that results from the lowering of local symmetry due to the distortion of the CoO_6 octahedra. By this we mean that a nearly cubic environment (though the actual symmetry is already orthorhombic) has a distortion that enhances the orthorhombic symmetry breaking. This corresponds to the more distorted octahedra that we find in the relaxed structures of the Co compounds, characterized by the parameter Δ_d (Table I).

We emphasize that here we performed standard GGA calculations and obtain these insulating states. This differs from calculations done with additional terms, such as in DFT + U methods, where an interaction that increases the separation of occupied and unoccupied d levels is applied [26]. Furthermore, we use the relaxed atomic positions obtained with standard GGA calculations, and still obtain a sufficient Jahn-Teller distortion to open a clean gap in the minority spin t_{2g} levels of the Co compounds, even for the ferromagnetic ordering. This is particularly remarkable considering that the orbital involved is Co d–O $p\pi$ antibonding t_{2g}, which generally may be expected to be much less Jahn-Teller active than the σ antibonding e_g orbitals.

IV. MAGNETISM

We now discuss the magnetic properties. Experiment shows all four compounds to be antiferromagnetic based on temperature dependent susceptibility measurements [11–13]. However, the particular magnetic order has not been established. The primitive unit cell contains four transition element atoms. Within one unit cell it is therefore possible to consider four collinear magnetic orders, denoted F, G, A, and C, and corresponding to ferromagnetic order, nearest neighbor antiferromagnetic order, ferromagnetic layers stacked antiferromagnetically along the crystallographic b axis, and nearest neighbor antiferromagnetic layers, stacked ferromagnetically along b to yield ferromagnetic chains along b, respectively. We calculated the total energy and electronic structures for all these orders, for each compound. These energies are given relative to the ferromagnetic order in Table II. The last row is the ratio of the experimental k_BT_N to the energy difference between the F and ground state G type orders. This energy difference is a measure of the average superexchange strength in a nearest neighbor model. In all cases the G-type order had the lowest energy, and all antiferromagnetic orders had lower energy than the ferromagnetic order. Within a nearest neighbor superexchange scheme, this shows that all the bonds of a metal atom to its six nearest neighbor metal atoms have antiferromagnetic coupling.

TABLE II. Magnetic energies $E_{\rm mag}$, in eV per formula unit, relative to the ferromagnetic ordering. No. AF is the number of antiferromagnetic nearest neighbors for each transition metal. The ratio on the last line is the ratio of the experimental k_BT_N [11–13] to the energy difference between the F and G orderings.

Order	No. AF	$CoSeO_3$	$CoTeO_3$	$NiSeO_3$	$NiTeO_3$
F	0	0	0	0	0
A	2	−0.0013	−0.0064	−0.0226	−0.0240
C	4	−0.0263	−0.0300	−0.0516	−0.0615
G	6	−0.0275	−0.0337	−0.0735	−0.0821
Ratio		0.15	0.20	0.11	0.13

In all cases and for all orders studied we find insulating gaps. Furthermore, in all cases, the fundamental band gap increased in going from the ferromagnetic to the antiferromagnetic ground state. Band gaps for the different orders are presented in the Supplemental Material, Table S2 [19]. The band gaps for the ground state antiferromagnetic G-type orders are indirect except for $CoTeO_3$, where the gap is direct. The Se compounds have larger band gaps than the corresponding Te compounds. Also the band gap increase with change of the order to antiferromagnetic is much stronger for the Ni compounds. In these Ni compounds the gap is between the occupied minority spin t_{2g} or majority e_g (for ferromagnetic) manifolds and the unoccupied minority e_g manifold and the increase amounts to ∼0.5 eV. In the Co compounds, the gap is between the lower and upper Jahn-Teller split t_{2g} submanifolds, and the increase amounts to less than 0.1 eV. This reflects the superexchange mechanism, which involves the e_g levels as discussed below. We note that the above places the magnetism in these compounds in the local moment (as opposed to the itinerant) limit.

As mentioned, all the compounds are antiferromagnetic, with a G-type ground state. Experimentally [11–13], the Néel temperatures, T_N, show considerable variation among these materials. The reported values are 49 K, 78 K, 98 K, and 125 K, for $CoSeO_3$, $CoTeO_3$, $NiSeO_3$, and $NiTeO_3$, respectively. It is of interest to develop understanding of these differences.

We begin with the structure. Subramanian and co-workers emphasized the importance of the metal-O-metal bond angles controlled by A-site size in explaining the crossover from antiferromagnetism to ferromagnetism in the $Cu(Se, Te)O_3$ alloy system. The Goodenough-Kanamori rules [27–29]

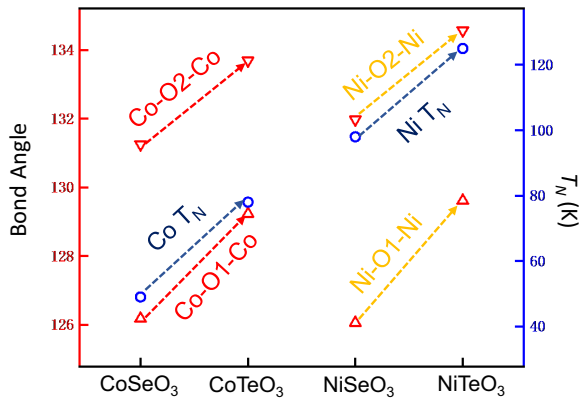

FIG. 4. Metal-O-metal bond angles from the relaxed structure and experimental Néel temperature, T_N, for the four compounds.

imply that the strongest antiferromagnetic tendency for these materials should be for straight bonds. In the present case, the perovskite framework is extremely distorted, with bond angles very far from the ideal 180°, and so the validity of extrapolating from the properties of mildly distorted perovskites may be questioned. However, the experimental T_N are indeed higher for the Te compounds than for the corresponding Se compounds. It is expected that the bonds will be straighter for Te than Se due to the larger size of Te. This is in fact the case based on our calculated structure data (Table I). Figure 4 shows the correlation between the two different bond angles and the experimental T_N for the Co and Ni compounds. This illustrates the trend, which is as expected from the Goodenough-Kanamori rules. Furthermore, while the T_N for the Ni compounds is consistently higher than for the Co compounds, this is not a consequence of different bond angles, e.g., from the smaller ionic radius of Ni, since in fact the bond angles are similar. It is also of interest to observe that the effect on the absolute T_N of comparable changes in bond angle is similar between the Co and Ni compounds.

Turning to the energies, it is notable that the energy difference between the ferromagnetic and G-type antiferromagnetic ground state follows the same order as the experimental values of T_N, i.e., $CoSeO_3 < CoTeO_3 < NiSeO_3 < NiTeO_3$. However, there is not a simple proportionality, which might be expected in an isotropic nearest neighbor Heisenberg model. Instead, the Co compounds show higher T_N than would be expected from scaling down the Ni compound values according to the F − G-type energy difference. This is seen in the ratios given in the last line of Table II.

This suggests a difference between the compounds, which is somewhat surprising due to the fact that the basic features of the electronic structure, especially as regards the e_g orbitals, are similar between the Co and Ni compounds. The e_g states are formally the σ antibonding d–O p combinations [27,29]. Therefore, with fully occupied majority e_g orbitals and unoccupied minority e_g orbitals, as in the present compounds, the strongest superexchange channel in perovskites involves the coupling of the e_g states, which as mentioned are similar between the four compounds.

One possible explanation could be in the chemical differences between Ni and Co, for example, different amounts of hybridization and different correlation strengths. One measure of the strength of hybridization that is readily available is the crystal field splitting. We focus on the minority spin in the ferromagnetic case, where the t_{2g} and e_g levels are separated from each other and from the O $2p$ bands. We obtain the center of the corresponding peaks in the density of states by integration of the first energy moment and thereby obtain the average minority spin crystal field splitting. In the Co compounds we include both subpeaks of the t_{2g} bands in the calculation of the average t_{2g} energy. The obtained crystal field splittings are 1.72 eV, 1.69 eV, 2.00 eV, and 1.97 eV, for $CoSeO_3$, $CoTeO_3$, $NiSeO_3$, and $NiTeO_3$. Thus the Ni compounds have larger crystal field splittings, indicating stronger hybridization. This may be the simple result of the fact that the Ni d states are closer in energy to the O $2p$ bands as seen in the projected densities of states (Figs. 2 and 3). In any case, it is consistent with stronger superexchange, since superexchange depends on metal-ligand hybridization [30]. This is as found in the present results. This type of superexchange due to e_g-e_g interactions with occupied t_{2g} orbitals increases the band gap for the antiferromagnetic state, since antiferromagnetism both narrows the bands and shifts the e_g level to higher energy. In the case of the Co compounds, the gap is between submanifolds of t_{2g} states. In this case band narrowing can increase the gap, but an upshift of the e_g level will not directly affect the gap, explaining the smaller band gap increases upon antiferromagnetic ordering in the Co compounds.

This is related to the possible explanation that strong correlations are present with different values of U that could be included in PBE + U calculations with U fit to experiment. However, while U generally can be used to reduce exchange couplings and fit T_N, and typically some U improves agreement with experiment in most transition metal oxides, it would be desirable to have a more first principles explanation if possible. Also, the apparently stronger hybridization in the Ni compound as indicated by the crystal field does not support a view that the Ni compound should have a larger U, since in general hybridization provides screening, which reduces the effective U. In any case, these results suggest that there may be a difference in the magnetic behavior also at the PBE level.

As mentioned, the local transition metal environment is more strongly distorted in the Co compounds due to the Jahn-Teller effect (note of course that the crystal symmetry is not cubic, and therefore that the local environment of the Co is always distorted in these compounds, meaning that the degeneracy of the Co t_{2g} levels is not exact to begin with). This leads to anisotropy in the exchange interactions. This can be seen in the pattern of energy differences in Table II. These energies are plotted in Fig. 5. The results show that the magnetic energy varies nearly linearly with the number of antiferromagnetic bonds in the Ni compounds. In contrast, antiferromagnetic bonds in the ac plane strongly lower the energy for the Co compounds. However, in the Co compounds the energy differences between the F and A order and between the C and G orders are small. This means that the b-axis interactions are comparatively quite weak. Consequently, while all the compounds have orthorhombic $Pnma$ symmetry, $NiSeO_3$

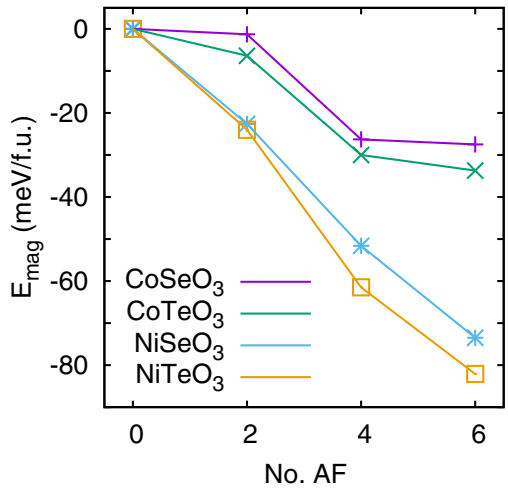

FIG. 5. Magnetic energy per formula unit defined as the energy difference from the ferromagnetic state for the F, A, C, and G type orders, which have 0, 2, 4, and 6 antiferromagnetic bonds per metal (No. AF), respectively. Note the different behavior of the Co and Ni compounds.

and $NiTeO_3$ are nearly isotropic from the point of view of their exchange interactions, but $CoSeO_3$ and $CoTeO_3$ are very anisotropic, and are more like layered materials from the point of view of exchange couplings. Based on the obtained energetics, the interactions in-plane are similar between the Ni and Co compounds (note especially the energy differences between A-type and C-type order, which probe this). Thus the Ni and Co compounds have very different anisotropy of the exchange interactions, and so a simple scaling of T_N with the F − G energy difference is not expected between the Co and Ni compounds.

V. SUMMARY, DISCUSSION, AND CONCLUSIONS

To summarize the results, we find, using standard density functional calculations at the PBE level, that these compounds are local moment antiferromagnetic insulators. The Ni compounds are insulating because of the narrow bands and sizable crystal field splitting. The Co compounds are also insulating due to a Jahn-Teller distortion of the octahedra. These calculations show near isotropic exchange interactions in the Ni compounds and a strong anisotropy with weak interactions along the b axis for the Co compounds. Remarkably, we find that these compounds are predicted to be insulators regardless of the specific magnetic order, even though we did standard PBE calculations.

A key characteristic of Mott insulators that distinguishes them from Slater insulators is the fact that both the ordered magnetic state and the higher temperature paramagnetic state are insulating with similar band gaps. This is a commonly applied experimental test for whether or not a material is a band insulator (i.e., Slater insulator) or a correlation driven Mott insulator. As discussed below, the present compounds mix these two categories as they satisfy the experimental test for a Mott insulator, but can do so for purely band structure reasons.

In local moment systems, such as the compounds discussed here, the phase transition is from an ordered antiferromagnetic state at low T to a high temperature paramagnetic state where the moments persist but are disordered. The spatial homogeneity of the paramagnetic state may then be regarded as due to temporal variations of the moments, that at any given time exist though without long range order. If the temporal variations are not too fast, one may approximate this state by thermodynamic averages over various disordered configurations. This is the so-called disordered local moment picture, which is very successful in describing both local moment materials and even materials such as iron that have some itinerant character [31–33]. Fully disordered static collinear moments (i.e., for an Ising case) could be simulated using methods such as the special quasirandom structure approach [34], though the present case may be more complex.

In the present selenite and tellurite compounds, all configurations have band gaps, with approximately similar values. Therefore, a gap is expected for any disordered configuration and therefore a disordered local moment picture will lead to gaps in the paramagnetic states. This includes the Co compounds where a Jahn-Teller distortion is present.

Thus these compounds present the unusual situation where one has local moment magnetism with insulating character that persists above the ordering temperature without the need for correlations beyond the standard PBE level. Recently, Zunger and co-workers [35–37] have used a closely related concept to explain properties of transition metal oxides, including monoxides and perovskites. They used special quasirandom structures to model the high temperature state. They did calculations allowing for local heterogeneity consistent with the quasirandom structures. However, in the work it was necessary to either include a correlation effect via a parameter U or to use a density functional such as SCAN that enhances the separation of occupied and unoccupied d levels, similar to a U parameter [38], leading to poor descriptions of itinerant magnets such as iron [39]. Another related option is the use of hybrid functionals, which incorporate mixing Hartree-Fock exchange, with various choices of the mixing and screening of the Coulomb potential [40–42]. Generally, these approaches can give insulating states in Mott insulators that are not properly described with standard PBE calculations. However, here we identify four bulk oxides, where the properties are characteristic of a Mott insulator, even at the level of standard PBE calculations, not including any additional correlation terms. This is not to say that the detailed agreement with experiments, when these become available, would not be improved by additional terms, such as U. However, our results point out an interesting possibility, realized in these compounds, that suggests further experimental investigations of their detailed properties, especially band gaps and spectra, as well as spin excitations. These may then be compared with theoretical results and used to constrain models. Spectroscopy in particular will be helpful in determining to what extent the band or Slater Mott-type insulating picture developed above is responsible for the properties of the materials, and conversely how important the Coulomb interactions are in determining the spectra.

Finally, we note that there are two distinct definitions of Mott insulators that are usually equivalent. These are

(1) the definition around the mechanism, specifically insulating character due to electron correlation induced localization and (2) the experimental definition related to persistence of the gap through the magnetic ordering temperature. While it is known that it is in principle possible to obtain behavior that meets the experimental test, without having the physics of the Mott mechanism, these compounds provide a rare example of dense, three dimensionally connected transition metal oxides that have this behavior.

ACKNOWLEDGMENTS

This paper results from work and analysis done by A.R.M.I., T.L., Q.L., A.M.M., M.V., and X.Z., in a project for the course "Structure, Electronic Structure and the Properties of Condensed Matter" in the Department of Physics and Astronomy at the University of Missouri, for which D.J.S. was the instructor. D.J.S. is grateful for support from the U.S. Department of Energy, Basic Energy Sciences, Grant No. DE-SC0019114, and for useful discussions with A. Zunger.

[1] M. A. Pena and J. L. G. Fierro, Chem. Rev. **101**, 1981 (2001).
[2] M. W. Lufaso and P. M. Woodward, Acta Crystallogr., B **60**, 10 (2004).
[3] J. G. Bednorz and K. A. Muller, Rev. Mod. Phys. **60**, 585 (1988).
[4] B. Jaffe, W. J. Cook, and J. Jaffe, *Piezoelectric Ceramics* (Academic, London, 1971).
[5] G. H. Jonker and J. H. van Santen, Physica (Amsterdam) **16**, 337 (1950).
[6] R. von Helmolt, J. Wecker, B. Holzapfel, L. Schultz, and K. Samwer, Phys. Rev. Lett. **71**, 2331 (1993).
[7] L. Malavasi, C. A. J. Fisher, and M. S. Islam, Chem. Soc. Rev. **39**, 4370 (2010).
[8] W. E. Pickett and D. J. Singh, Phys. Rev. B **53**, 1146 (1996).
[9] T. Kimura, T. Goto, H. Shintani, K. Ishizaka, T. Arima, and Y. Tokura, Nature (London) **426**, 55 (2003).
[10] D. I. Khomskii and G. A. Sawatzky, Solid State Commun. **102**, 87 (1997).
[11] K. Kohn, S. Akimoto, Y. Uesu, and K. Asai, J. Phys. Soc. Jpn. **37**, 1169 (1974).
[12] K. Kohn, K. Inoue, O. Horie, and S. Akimoto, J. Solid State Chem. **18**, 27 (1976).
[13] K. Kohn, S. Akimoto, K. Inoue, K. Asai, and O. Horie, J. Phys. Soc. Jpn. **38**, 587 (1975).
[14] L. Pauling, J. Am. Chem. Soc. **51**, 1010 (1929).
[15] M. A. Subramanian, A. P. Ramirez, and W. J. Marshall, Phys. Rev. Lett. **82**, 1558 (1999).
[16] D. J. Singh and L. Nordstrom, *Planewaves Pseudopotentials and the LAPW Method*, 2nd ed. (Springer, Berlin, 2006).
[17] P. Blaha, K. Schwarz, G. Madsen, D. Kvasnicka, and J. Luitz, *WIEN2k, An Augmented Plane Wave + Local Orbitals Program for Calculating Crystal Properties* (K. Schwarz, Tech. Univ. Wien, Austria, 2001).
[18] J. P. Perdew, K. Burke, and M. Ernzerhof, Phys. Rev. Lett. **77**, 3865 (1996).
[19] See Supplemental Material at http://link.aps.org/supplemental/10.1103/PhysRevB.101.045107 for structural details and band gaps.
[20] R. D. Shannon, Acta Crystallogr., A **32**, 751 (1976).
[21] J. Alonso, M. Martinez-Lope, M. Casais, and M. Fernandez-Diaz, Inorg. Chem. **39**, 917 (2000).
[22] M. R. Michel, Ph.D. thesis, University College London, 2010.
[23] C. J. Honer, M. J. Prosniewski, A. Putatunda, and D. J. Singh, J. Phys.: Condens. Matter **29**, 405501 (2017).
[24] J. C. Slater, Phys. Rev. **82**, 538 (1951).
[25] K. Terakura, T. Oguchi, A. R. Williams, and J. Kubler, Phys. Rev. B **30**, 4734 (1984).
[26] V. I. Anisimov, F. Aryasetiawan, and A. I. Lichtenstein, J. Phys.: Condens. Matter **9**, 767 (1997).
[27] J. B. Goodenough, J Phys. Chem. Solids **6**, 287 (1958).
[28] J. Kanamori, J. Phys. Chem. Solids **10**, 87 (1959).
[29] J. B. Goodenough, *Magnetism and the Chemical Bond* (Wiley, New York, 1963).
[30] P. W. Anderson, Phys. Rev. **79**, 350 (1950).
[31] J. B. Staunton and B. L. Gyorffy, Phys. Rev. Lett. **69**, 371 (1992).
[32] J. Mizia, J. Phys. F: Met. Phys. **12**, 3053 (1982).
[33] J. B. Staunton, Rep. Prog. Phys. **57**, 1289 (1994).
[34] A. Zunger, S. H. Wei, L. G. Ferreira, and J. E. Bernard, Phys. Rev. Lett. **65**, 353 (1990).
[35] G. Trimarchi, Z. Wang, and A. Zunger, Phys. Rev. B **97**, 035107 (2018).
[36] J. Varignon, M. Bibes, and A. Zunger, Nat. Commun. **10**, 1658 (2019).
[37] J. Varignon, M. Bibes, and A. Zunger, Phys. Rev. B **100**, 035119 (2019).
[38] Y. Fu and D. J. Singh, Phys. Rev. B **100**, 045126 (2019).
[39] Y. Fu and D. J. Singh, Phys. Rev. Lett. **121**, 207201 (2018).
[40] J. Heyd, G. E. Scuseria, and M. Ernzerhof, J. Chem. Phys. **118**, 8207 (2003).
[41] J. Heyd, G. E. Scuseria, and M. Ernzerhof, J. Chem. Phys. **124**, 219906 (2006).
[42] A. V. Krukau, O. A. Vydrov, A. F. Izmaylov, and G. E. Scuseria, J. Chem. Phys. **125**, 224106 (2006).